Shear rate gradients promote a bi-phasic thrombus formation on weak adhesive proteins, such as fibrinogen in a von Willebrand factor-dependent manner

Nicolas Receveur,[1]* Dmitry Nechipurenko,[2,3,4]* Yannick Knapp,[5,6] Aleksandra Yakusheva,[2,3,4] Eric Maurer,[1] Cécile V. Denis,[7] François Lanza,[1] Mikhail Panteleev,[2,3,4] Christian Gachet[1] and Pierre H. Mangin[1]

[1]Université de Strasbourg, INSERM, EFS Grand-Est, BPPS UMR-S1255, FMTS, Strasbourg, France; [2]Faculty of Physics, Moscow State University, Moscow, Russia; [3]Federal Research and Clinical Centre of Pediatric Hematology, Oncology and Immunology, Moscow, Russia; [4]Center for Theoretical Problems of Physicochemical Pharmacology, Moscow Russia; [5]CNRS, Université Aix-Marseille, Ecole Centrale Marseille, IRPHE UMR7342, Marseille, France; [6]Université Avignon, LAPEC EA4278, Avignon, France and [7]HITh, UMR_S1176, INSERM, Université Paris-Sud, Université Paris-Saclay, Le Kremlin-Bicêtre, Paris, France

*NR and DN contributed equally as co-first authors

Supplemental Materials and methods

Materials

Recombinant hirudin was from Transgene (Illkirch-Graffenstaden, France), acid citrate dextrose (ACD) solution from Bioluz (St-Jean-de-Luz, France). Apyrase was purified from potatoes as previously described [1], prostaglandin E1 (PGE1), fatty acid-free human serum albumin (HSA) and human fibrinogen were purchased from Sigma-Aldrich (St. Louis, MO). Polydimethylsiloxane (PDMS) and curing agent from Dow Corning (Midland, MI). $DiOC_6$ (3,3'-dihexyloxacarbocyanine iodide) was from Molecular Probes (Paisley, UK). Human VWF was isolated from factor VIII concentrates (EFS-Alsace, Strasbourg, France) as previously described [1].

Mice

C57BL/6 Wild-type (WT) were purchased from Charles River (L'Arbresle, France). Von Willebrand Factor-deficient ($VWF^{-/-}$) mice on a pure C57BL/6 genetic background were generated by Cécile Denis [2]. The mice were maintained in the animal facilities of the Etablissement Français du Sang Grand-Est. Ethical approval for animal experimentation was obtained from the French Ministry of Research in accordance with the European Union Guidelines as defined by European laws.

Antibodies and synthetic peptides

The human integrin αIIbβ3 antagonist, abciximab (ReoPro®), was purchased from Lilly (Indianapolis, IN, USA). The GPIIb-IIIa antagonist eptifibatide (Integrilin®) was obtained from Millennium Pharma (San Francisco, CA) and anti-human GPIbα, AK.2, was from GeneTex (Euromedex, Souffelweyersheim, France). The anti-human GPIbα peptide OS-1 and its scrambled control version were synthesized by PolyPeptide Laboratories (Strasbourg, France). Anti-human VWF A1 domain, clone 701, was kindly provided by Dr. C.V. Denis [3]. Anti-VWF was purchased from Agilent-DAKO (Les Ulis, France) labeled with Alexa 488 Antibody labeling kit from ThermoFisher Scientific (Illkirch, France).

Preparation of washed platelets and reconstituted blood

Human blood samples were collected from healthy volunteers abstained from drugs known to affect platelet function, for at least 10 days [1]. 50 mL of blood were collected into acid citrate dextrose (1:7[v/v]) or hirudin (100 U/mL), gently mixed and kept at 37°C. ACD-anticoagulated whole blood was centrifugated at 250 g for 16 min to obtain platelet rich plasma (PRP) and washed by sequential centrifugation, as previously described [1]. Washed platelet suspensions were resuspended at a concentration of 3 x 10^{11} platelets/L in Tyrode's albumin buffer containing 0.02 U/mL apyrase. To prepare reconstituted blood, whole blood was centrifuged at

250 x g for 16 min and after removal of the supernatant PRP and the buffy coat layer the remaining red blood cells were washed twice in Tyrode's buffer and treated with 0.02 U/mL apyrase prior to reconstitution with autologous washed platelets (50% (v/v)) at final concentration of 250 x 10^6 platelets/mL.

In Vitro flow-based studies

Flow-based assays were performed as previously described [4]. Briefly, microfluidic channels were coated with a fibrinogen solution (300 µg/mL) overnight at 4°C and blocked with human serum albumin (HSA) in Phosphate buffered saline (PBS) 0.5% for 30 min at RT. Hirudinated (100 U/mL) whole blood was perfused at 37°C through the coated channels at the indicated WSR with a programmable syringe pump (PHD 2000, Harvard Apparatus, Holliston, MA, USA). In some sets of experiments, hirudinated whole blood was preincubated with indicated concentrations of Reopro®, Integrilin®, AK.2, Scramble, OS-1 or anti-VWF A1 domain for 15 minutes at 37°C before perfusion. Platelet adhesion was visualized using differential interference contrast (DIC) microscopy images obtained with an inverted Leica DMI 4000 B microscope (Leica Microsystems, Manheim, Germany: 40x, 1.4 numerical aperture oil lense) coupled to complementary metal-oxyde semiconductor (CMOS) camera (ORCA-Flash4.0 LT, Hamamatsu, Massy, France). For quantification of platelet accumulation onto fibrinogen, whole blood was labeled with 1 µmol/L $DiOC_6$ for 15 min at 37°C, perfused through the coated channel and platelet adhesion was monitored using epifluorescence and DIC combination microscopy. Data were recorded for offline analysis using Metamorph software version 7.7 (Molecular Devices, Downingtown, PA, USA) or ImageJ software (National Institutes of Health). For Confocal microscopy, thrombus and VWF fibers were visualized with an inverted Leica SP8 microscope (Leica Microsystems, Manheim, Germany) and analyzed with ImageJ software.

Micro-particle image velocimetry (microPIV)

In order to assess experimentally the flow in different regions of the model, 2D velocity fields were measured in different planes along the height of the model using micro particle image velocimetry, microPIV [5]. Since this technique needs a transparent working fluid, a 40/60 Glycerol/PBS mixture served as a blood mimicking fluid. Viscosity measurements with a Haake Mars III rheometer (Thermo Fisher Scientific, France) resulted in a dynamic viscosity of 3.5 mPa.s which is typical of blood viscosity at high shear rates. The mixture was seeded with 1 µm fluorescent particles (FluoSpheres F8819, Invitrogen, France) which match the specificities of the filter cube implemented in the inverted episcopic microscope (Olympus IX71, Olympus, France) used for these experiments. The mixture was fed to the flow chamber under the same conditions than for the *in vitro* flow based studies (37°C). The flow generated in the model was illuminated in volume by a double-pulsed 532 nm laser light (NdYag Gemini PIV, New Wave Research, USA). The 575 fluorescing particles were then imaged with a 12-bit cooled 1.4 Mpixel digital CCD camera system (Sensicam, PCO, Germany). The thickness of the velocity plane was determined from the computation of the Depth of Correlation [5] which was 10.4 µm for the experiments realized with an UPLFLN 20X microscope lens. At such magnification, the field of view was 907 x 676 µm. Measurements were performed in 15 planes

equally distributed over the 100 µm channel height with a constant in 7.33 µm separation between planes. As a principle of the method, laser synchronized images pairs were acquired and the displacement in small rectangular 50% overlapping windows was determined by means of a FFT based correlation computation. As a specificity of microPIV, since the tracer seeding density is low, a correlation averaging computation is implemented over sets of 20 image pairs [5]. The resulting spatial resolution of the method was 5.28 x 10.56 µm in the x and y directions respectively. Such resolution allowed a close comparison with analytical solutions of the flow in the straight channels of the microfluidic chamber and with Computational fluid dynamic (CFD).

Computational fluid dynamics

Flow hydrodynamics inside the flow chambers was calculated with Comsol 5.4 (Comsol, Burlington, MA) package using stationary laminar flow hydrodynamics module. Laminar inflow of $5 \ 10^{-10}$ m^3/s (30 µL/min) and outlet with zero pressure were used as boundary conditions for inlet and outlet, respectively. No slip boundary conditions were chosen for other surfaces of the flow chamber. Newtonian liquid model with viscosity of 3 mPa.s was chosen for the fluid. Shear rates and elongation rates in the center line of the flow chamber were calculated based on corresponding velocity derivatives. Shear rate at the center line of the chamber wall of the stenosed part of the chamber was also calculated from analytical solution Navier-Stokes equation for infinitely long channel with square-shaped geometry and corresponding volumetric flow rate. In order to estimate the shear rates above single adhered platelets in zone 3 (**Figure 1E**), only a small part of rectangular zone 3 was considered: 300 x 100 x 100 µm were the xyz dimensions of computational domain. Several ellipsoids (with 1 and 2 microns for z and x (y) – axis) mimicking single adhered platelets were placed near the wall of the chamber with their centers lying in the central z-x plane. In order to illustrate the flow lines compression effect one ellipsoid was placed higher mimicking the second layer-platelet. Shear rates and flow lines were visualized using the standard Comsol functions.

To calculate the flow field inside the stenosed vessel, the vessel was considered as a cylinder with 250 µm radius and 5 000 µm length (x-axis). The ellipsoid (with 1 353 microns in x and 400 microns in y and z dimensions) mimicking stenosis was placed with its long axis coincident with the bottom of the cylinder (**Figure 6**). Laminar inflow of $25 \ 10^{-3}$ m/s (0.6 mL/min) and outlet with zero pressure were used as boundary conditions for inlet and outlet, respectively. The flow value was derived using the constant-pressure drop model, validated using the experiments of the FeCl$_3$-induced thrombosis with Doppler probe (**data not shown**). No slip boundary conditions were chosen for other surfaces of the vessel. Shear rates, shear rate gradients and flow lines were visualized using the standard Comsol functions.

In Vitro **Binding Assay**

96-well ELISA plates were incubated overnight at 4°C with PBS-20 mg/mL BSA or with carbonate buffer (pH 9.6) containing fibrinogen (5 µg/mL). After blocking with PBS-20 mg/mL BSA for 1h at 37°C, increasing concentrations of human VWF (5 µg/mL) in blocking solution

(1:1,000 Tween 20, 1 mg/mL BSA, 0.5 mmol/L $MgCl_2$ and 1 mmol/L $CaCl_2$ in PBS) were added to the coated wells for 2 h at 37°C. To detect bound VWF, an HRP-conjugated anti-VWF antibody (0.4 µg/mL in blocking solution) was added for 1 h at room temperature. O-phenylenediamine was then added for 5 min, after which the reaction was discontinued with 50 µL of 3 mol/L H_2SO_4 and the plates were read at 490 nm.

Defining shear rate gradients and elongation rate of the flow

The WSR changes throughout zone 2 – increasing from 300 s^{-1} at zone 1 to approximately 4,800 s^{-1} at zone 3. In order to address the definition of shear rate gradient in this work, we focused at the central x-z plane of the chamber. The WSR throughout the central line of the chamber floor is defined as $\dot\gamma = \frac{\partial v}{\partial z}$, where v is the value of local flow velocity (in the z-x plane flow velocity has only x component). The SRG value is described here as the magnitude of $\frac{\partial \dot\gamma}{\partial x}$ – thus, it shows how fast does the WSR change in the direction of the flow (x-axis). It should be noted, the value of SRG also characterizes the value of flow acceleration above the chamber floor: the velocity gradient along the direction of the flow $\varepsilon = \frac{\partial v}{\partial x}$ at some height h above the chamber floor can be approximated by the formula $\varepsilon = \frac{\partial \dot\gamma}{\partial x} h$. This velocity gradient ε along the direction of the flow is also termed elongation rate. Thus, SRG value shows how fast the elongation rate grows with height above the surface at which SRG is defined. SRG values given below correspond to the maximum values of SRG which take place just at the entrance of zone 3.

Statistical analysis

All statistical analyses were performed using GraphPad Prism program, version 5.0 (Prism, GraphPad, LaJolla, CA, USA). All values are reported as mean ± standard error of the mean (S.E.M.). The distribution of the data was evaluated by D'Agostino-Pearson test; parametric or non-parametric tests were used as appropriate. Data between two groups were compared by the Mann-Whitney test while for comparison among multiple groups, one-way ANOVA or Friedman test.

References

1.   Cazenave JP, Hemmendinger S, Beretz A, Sutter-Bay A, Launay J. [Platelet aggregation: a tool for clinical investigation and pharmacological study. Methodology]. *Ann Biol Clin (Paris)*. 1983;41(3):167-179.
2.   Denis C, Methia N, Frenette PS, et al. A mouse model of severe von Willebrand disease: defects in hemostasis and thrombosis. *Proc Natl Acad Sci U S A*. 1998;95(16):9524-9529.

3.   Obert B, Houllier A, Meyer D, Girma JP. Conformational changes in the A3 domain of von Willebrand factor modulate the interaction of the A1 domain with platelet glycoprotein Ib. *Blood*. 1999;93(6):1959-1968.

4.   Maurer E, Schaff M, Receveur N, et al. Fibrillar cellular fibronectin supports efficient platelet aggregation and procoagulant activity. *Thromb Haemost*. 2015;114(6):1175-1188.

5.   Wereley S, Meinhart C. Recent Advances in Micro-Particle Image Velocimetry. *Annual Review of Fluid Mechanics*. 2010;42(1 January 2010):557-576.

Supplemental Figure 1

A.   PDMS Chamber

3D view

Straight
Channel
1 mm

Straitght 0.1
Channel
100 µm
100 µm

Top view

Straight
Channel
1 mm

Straitght 0.1
Channel
100 µm
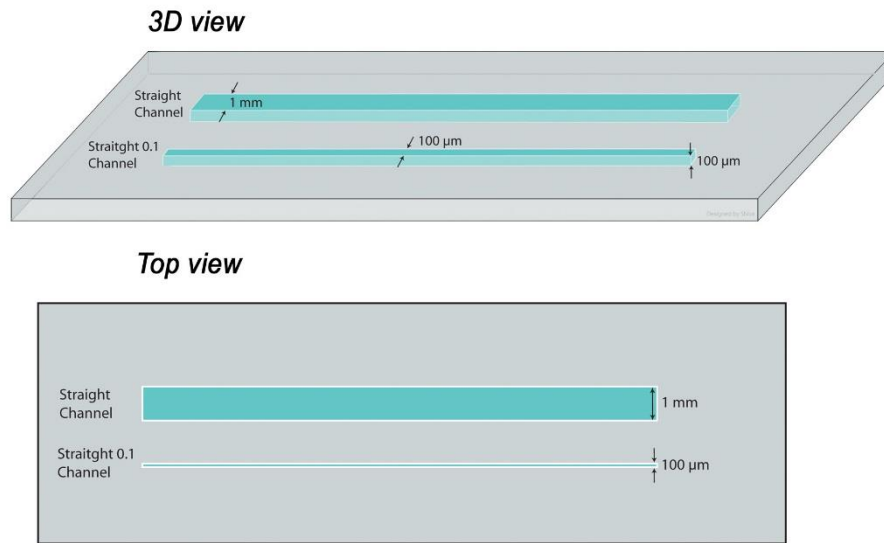
Supplemental figure 1. Schematic of the straight narrowed flow chamber. A, Schematic of the PDMS-based microfluidic flow chamber containing a straight rectangular channel with a width of 0.1 mm and a height of 0.1 mm.

Supplemental Figure 2
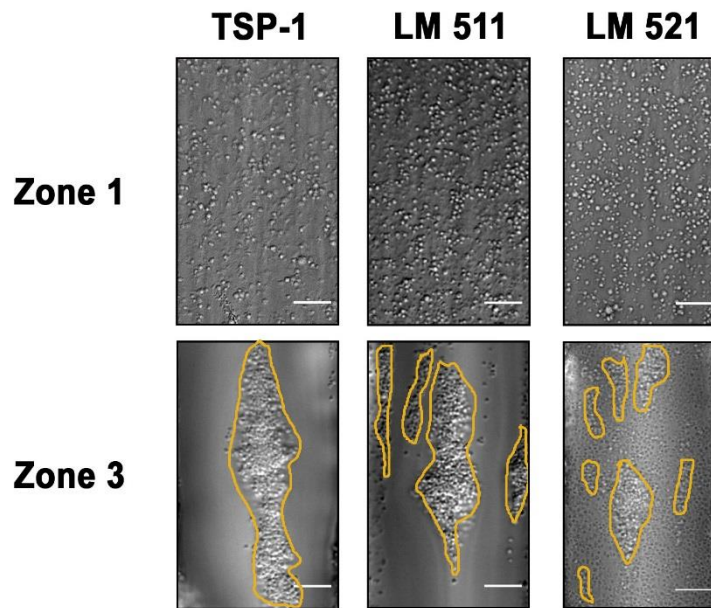
Supplemental figure 2. Platelet accumulation and agregation in the stenosed channel on thrombospondin and laminins. Hirudinated human whole blood was perfused through channels coated with a solution of 100 µg/mL of thrombospondin-1 (TSP-1) or Laminins 511 or 521 (LM511 or LM521). Representative DIC images of platelets adhering or aggregating in zone 1 and zone 3 of the stenosed 90% channel, after 5 min. Scale bar : 10 µm.

Supplemental Figure 3

A.

B.
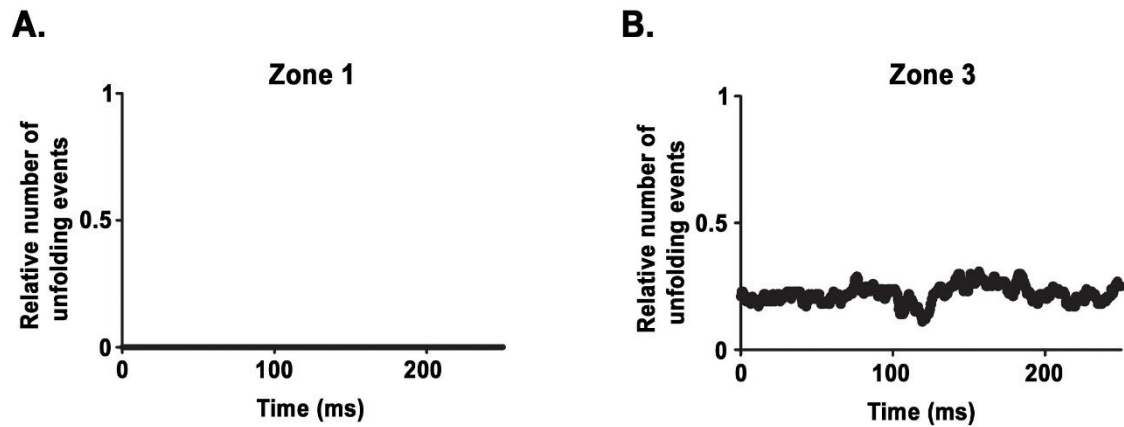
Supplemental figure 3. Comparison of VWF unfolding events in different zones of the flow chamber with stenosis. The relative number of vWF unfolding events above the fibrinogen surface was determined by Computational modeling of vWF dynamics using the CFD-derived values of shear rates in zone 1 (shear rate of 300 s^{-1}) and zone 3 (shear rate of 4800 s^{-1}). For each zone 100 simulations of long vWF multimers dynamics were obtained. VWF molecule was considered unfolded only if its maximal size exceeded contour length of the multimer.

LEGENDS TO VIDEOS

Supplemental video 1. SRGs promote platelet aggregation on a fibrinogen surface which leads to channel occlusion. Hirudinated human whole blood was perfused through channels of the stenosed microfluidic chamber coated with a solution of fibrinogen (300 μg/mL). The video shows representative sequences of DIC images of platelets accumulating to immobilized fibrinogen at the entry of zone 3 (4,800 s^{-1}). Channel occlusion is observed. Scale bar: 10 μm.

Supplemental video 2. Bi-phasic thrombus formation in the stenosed region under SRGs. Hirudinated human whole blood was perfused through channels of the stenosed microfluidic chamber coated with a solution of fibrinogen (300 μg/mL). The video shows representative sequences of DIC images of platelets accumulating to immobilized fibrinogen at the entry of zone 3 (4,800 s^{-1}). The process is biphasic. Scale bar: 10 μm.

Supplemental video 3. VWF multimer unfolding during its movement through zone 2-zone 3. Simulation of long vWF multimer during it's entrance to zone 3 through zone 2. Video corresponds to one of the 100 trajectories obtained for long (80 dimers) vWF molecule traveling 10 microns above the fibrinogen surface. The position of the multimer inside the chamber (x-y section) is shown in the lower part of the video. This simulation covers vWF dynamics as it travels 1 millimeter through the end of zone 2 and over 2 millimeters in zone 3.

Supplemental video 4. VWF fiber formation occurs before thrombus growth under SRGs. Hirudinated human whole blood was perfused through channels of the stenosed microfluidic chamber coated with a solution of fibrinogen (300 μg/mL). The video shows representative sequences of DIC/fluorescent images of platelets and VWF (green) accumulating to immobilized fibrinogen at the entry of zone 3 (4,800 s^{-1}). Scale bar: 20 μm.

Supplemental video 5. Thrombus growth is accelerate under SGRs in an injured mouse carotid artery. The common carotid arteries of adult mice were exposed and a filter paper saturated with 4% $FeCl_3$ was placed laterally on the left vessel for 2.5 min. After 4 min, the vessel was pinched with a micromanipulator to realize an > 80% stenosis. The video shows representative sequences of fluorescent images of a thrombus forming after vessel injury obtained by labeling the platelets with $DIOC_6$. Scale bar: 100 μm.